



A Single Stage New Multi-Port Power Converter for Electric Vehicle Applications

1Dr.G.V.Prasanna Anjaneyulu 2s.vasundara, 3shailk Kasim ,

4y Sirisha, 5n.bhanu sri

1Associate Professor , 2,3,4,5 UG Scholars Department of Electrical & Electronics Engineering, R.V.R.&J.C college Engineering & Technology, Guntur, Andhra Pradesh Email: eeer.v.r.j.c@gmail.com

Abstract—This work presents the design and implementation of a non-isolated single inductor multiport DC-DC Converter for electric vehicle(EV) applications , aimed at integrating multiple energy sources such as solar photovoltaic (PV) and battery system. The proposed converter architecture offers a simplified , cost-effective solutions with reduced component count, ensuring flexible and efficient power management for hybrid energy systems. The converter is capable of dual input and dual output operations, allowing bidirectional energy flow with appropriate control strategies to manage charging and discharged modes. Designed using MATLAB/Simulink and validated through hardware experimentation, the system dynamically regulates output voltages and battery currents even under varying load and reference conditions

I. INTRODUCTION

The growing global demand for energy, coupled with the depletion of fossil fuels and rising environmental concerns, has accelerated the shift toward electric vehicles (EVs) powered by renewable energy sources. Among these, solar photovoltaic (PV) systems are increasingly integrated into EV powertrains to offer a clean and sustainable energy alternative. However, due to the intermittent nature of solar energy, hybrid systems combining PV and battery storage have become essential to ensure continuous and reliable power supply. Traditional multi-input converters used in such systems often involve complex and bulky circuitry. To address these limitations, this research introduces a non-isolated single inductor multi-port converter that simplifies the system design while enabling efficient energy sharing between multiple inputs and outputs. This converter supports flexible operation modes for both charging and discharging, offering a compact, cost-effective solution for next-generation EV applications, used to interface energy storage systems such as batteries and supercapacitors. Implementing the system with the system's cost. As a result, a converter with multiple voltage-rated inputs is required to handle multiple energies and feed them into the system. In general, hybrid energy storage systems are interfaced with a multi-input converter, which comes in a variety of variants depending on the Isolation requirement for non-isolation and isolation type DC-DC converters. FIGURE 1 depicts the general layout of the multi- input converter-fed electric motor.

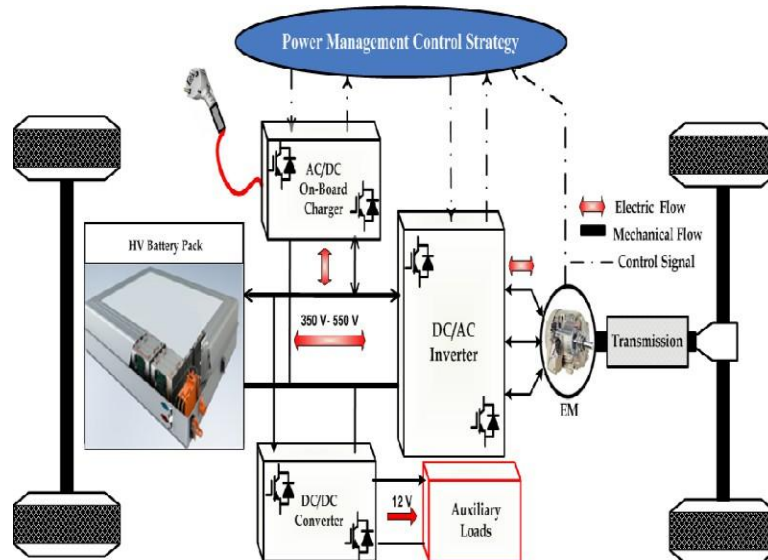


Figure 1: Block diagram of the BEV powertrain

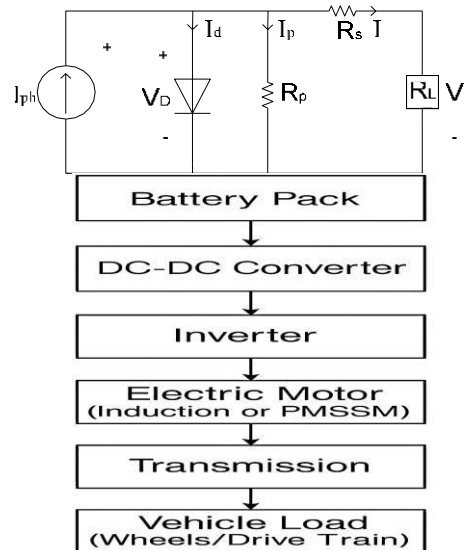
In an isolated multi-port converter configuration, a high-frequency transformer is used to produce isolation between the electric constraints. This allows for efficient isolation and impedance matching on both sides of the converter. Leakage inductance is used as a storage device in isolated converters to transmit power between both sides of the converter. Isolated dc-dc converters frequently include power converters in addition to the high-frequency transformer. The transformer phase shift between the primary and secondary voltage constraints has been changed to maintain efficient power transfer from both converter ports [9], [10], [11]. There are several types of converters in this category, including half-bridge converters, full-bridge converters, and combinational multiport converters [12], [13], [14]. Because of the transformer, these are quite large. Inverters are required in these converters at the transformer's input port, with which dc can be converted to ac supply and ac can be converted to dc using the converters. As a result, various switches are used in all converter terminals, increasing the losses, and the system losses increase as transformer winding losses increase. These shortcomings are addressed in non-isolated multi-port converters, which are ideal for electric vehicle applications.

Concerning the H-bridge, a non-isolated multiport converter has been implemented [15]. In practice, various voltages can be obtained by cascading H-bridge configurations while taking into account various dc-link voltage levels. Because of the converter's coupling mechanism to multiple ports, the negative modes are not investigated [16], [17] Introduces the concept of a multiphase converter. The energy stored in the converter's energy storage sources can be absorbed as well as delivered to the load. There exists an individual inductor for each source and hence this is considered a drawback of the converter [18], [19], [20] also cost-efficient three-port converter for EV/HEV applications is proposed The author offers a three-input converter for the connection of batteries, solar cells, and fuel cells [21].



You can charge and discharge the battery from various sources and loads with proper converter switching. Reference [22] Presents a systematic method for designing non-isolated topologies using a combination of buck, boost, sepic, and cuk type converters. There are two types of converters described: PVSC and PCSC, which are pulsing voltage and current sources. As a voltage source, PVSC can be connected in series with an inductor to form a double input converter. Because the PCSC is a current source, it may be used to build a double- input converter by connecting it in series with a capacitor. In [20], the energy management strategy among the various inputs like battery, SC and the electric motor is suggested for use in an electric automobile. Here, instead of employing two separate inductors as energy storage components are used. When compared to two independent inductors, it is claimed that employing the inductors with coupling can able to save 22–26% in volume. In contrast, connected inductors have a larger volume than a single inductor. This converter can also regenerate braking energy to the battery and SC. Reference [23] proposes transferring load power across input sources using a multiport converter with a single inductor. This converter can also be used to transfer power from one source to another. In [24], the author introduced a novel zero voltage switching DC-DC converter. The layout of conventional converters utilized in electric vehicles is represented in FIGURE 2 (a) whereas the proposed converter configuration is represented in FIGURE 2 (b).

Connected inductors, on the other hand, have a larger volume than a single inductor. This converter also allows for the regeneration of braking energy to the battery and SC. Reference [23] suggests transferring load power across input sources using a multiport converter with a single inductor. This converter can also be used to transfer power between sources. References [25] and [26] offer a multi-port converter that may create numerous voltages at its output sections and these are the preset values regardless of the variation of the load power and input voltage interfaced with PV systems. Reference [27] Presents a novel multi-output buck converter control technique that delivers suitable dynamic performance. However, this converter is worthless in applications like electric cars, where various input energy excitations like solar and a battery are utilized. This can be solved by incorporating multi-port converters. Reference [28] Describes a non-isolated high step-up multi-port converter and its performance evaluation using a variety of parameters. References [29] and [30] evaluate the MPPT of a solar PV converter under partial shading conditions. Another advantage in the proposed converter is its inability to transmit energy across input sources. A multi-port non-isolated converter is suggested in this work, which is based on the mixture design of multiple inputs and outputs of the converter. In comparison to previous scenarios, the suggested converter contains fewer components. This converter can regulate the flow of electricity between sources and loads. Furthermore, the suggested converter includes many outputs, each of which can have a different voltage level. The remainder of the paper is presented as follows. Section II provides the modeling of solar PV and MPPT. Section III explains the construction and modes of operation of the developed converter. The dynamic modeling is shown in Section IV. Whereas the control architecture of the converter is discussed in section V. Both simulation and experimental results are discussed in Sections VI and the article is concluded in Section VII.



In this section, an elaborate mathematical modeling and simulation study of a PV cell are presented. The solar cell is the most basically a semiconductor diode disposed to irradiance. The solar cells are made up of semiconductor by using the different procedure of production [16]. Solar irradiance consists of photons containing different levels of energy, some of which are absorbed in the p-n junction. The photons with the energy less than the bandgap of the solar cell are useless. Those photons can't generate the voltage and the electrical current. The photons, which have much more energy than the bandgap, generate energy but the energy is only used at a level equal to the bandgap. The remaining energy is dissipated as heat in the body of the PV cell [17-18]. The equivalent circuits commonly used for modelling of a PV cell are known as single-diode and two-diode models. The single-diode and two-diode models of a PV cell are as shown in Fig.1 and Fig.2 respectively. The two-diode equivalent circuit has a more complex structure and exhibits more nonlinear characteristics than the single-diode equivalent circuit. Therefore two-diode models are rarely used. Single-diode models are commonly used models as a good trade-off between accuracy and simplicity [4,19,20]. In this paper, single-diode equivalent circuit model is preferred, and DS-100 M PV module is taken as reference model for practical comparison. The DS-100 M PV module datasheet parameters are given as rated power 100W, voltage at maximum power point (MPP) 18V, current at MPP 5.55A, open circuit voltage 21.6V, short circuit current 6.11A, the number of cells in series (N_s) 36, the number of cells in parallel (N_p) 1, maximum system voltage 1000V, the short circuit current/temperature coefficient (K_i) 0.002 and range of operation temperature $-40^\circ\text{C} - 80^\circ\text{C}$. The datasheet parameters of a PV module are given at standard test conditions (STK; 25°C and 1000 W/m^2) [18].



the voltage and current generated by the PV array. As a result, it is necessary to make an informed decision on the sort of solar panel to choose. increase the dynamic behavior and performance of the MPPT. Artificial intelligence techniques that focus on the nonlinear features of PV arrays provide a speedy but computationally challenging solution to the MPPT issue. The indirect methods function by calculating the arrays MPP based on the output characteristics. The open-circuit voltage OCV and the short-circuit current SCC .

$$I=I_{ph}-I_0\left(\exp\left(\frac{q(V+IR_s)}{kT}\right)-1\right)-R_{sh}V+IR_s\text{..... (1)}$$

The modeling of a photovoltaic (PV) cell is essential to analyze and predict its behavior under various environmental conditions, such as sunlight and temperature. A PV cell converts solar energy directly into electrical energy based on the **photovoltaic effect**. The electrical equivalent model of a PV cell is typically represented using a **current source, diode, series resistance, and shunt resistance**.

III. MPPT with Artificial Neural Networks (ANN) for Solar-Powered Systems

Maximum Power Point Tracking (MPPT) is a critical technology in solar energy systems, ensuring that photovoltaic (PV) panels operate at their optimal efficiency despite varying environmental conditions like irradiance and temperature. Traditional MPPT methods, such as Perturb and Observe (P&O) and Incremental Conductance (INC), rely on predefined algorithms to track the maximum power point (MPP). However, these methods often struggle with rapid changes in weather conditions, leading to oscillations around the MPP or slow convergence. To address these limitations, **Artificial Neural Networks (ANNs)** have emerged as an advanced solution for MPPT, leveraging machine learning to predict and adapt to dynamic solar conditions with higher accuracy and speed.

ANNs are particularly effective in MPPT because they can **learn and model nonlinear relationships** between input parameters (e.g., solar irradiance, temperature, and panel voltage/current) and the corresponding MPP. A well-trained ANN processes real-time sensor data and predicts the optimal operating point almost instantaneously, eliminating the oscillations seen in conventional methods. The ANN-based MPPT system typically consists of **three phases**: (1) **Data Collection**, where historical and real-time PV system data are gathered; (2) **Training**, where the ANN learns the relationship between environmental inputs and the MPP using algorithms like backpropagation; and (3) **Implementation**, where the trained ANN is deployed in the MPPT controller to adjust the DC-DC converter's duty cycle dynamically.

One of the key advantages of ANN-based MPPT is its **robustness under partial shading conditions**, where traditional methods often fail due to multiple local maxima in the power-voltage curve. By training the ANN on diverse shading scenarios, the system can distinguish between global and local peaks, ensuring maximum energy harvest. Additionally, ANNs reduce computational overhead compared to complex optimization algorithms, making them suitable for **low-cost embedded systems** like Arduino or Raspberry Pi-based MPPT controllers.



Despite its benefits, ANN-based MPPT faces challenges such as the **need for extensive training data** and occasional retraining to adapt to long-term panel degradation or climate variations. However, with advancements in **edge AI and real-time learning**, these systems are becoming more adaptive and scalable. Future research focuses on hybrid approaches, combining ANNs with fuzzy logic or reinforcement learning, to further enhance efficiency in fluctuating environments. In summary, ANN-based MPPT represents a **smart, adaptive, and high-performance alternative** to conventional methods, paving the way for next-generation solar energy systems.

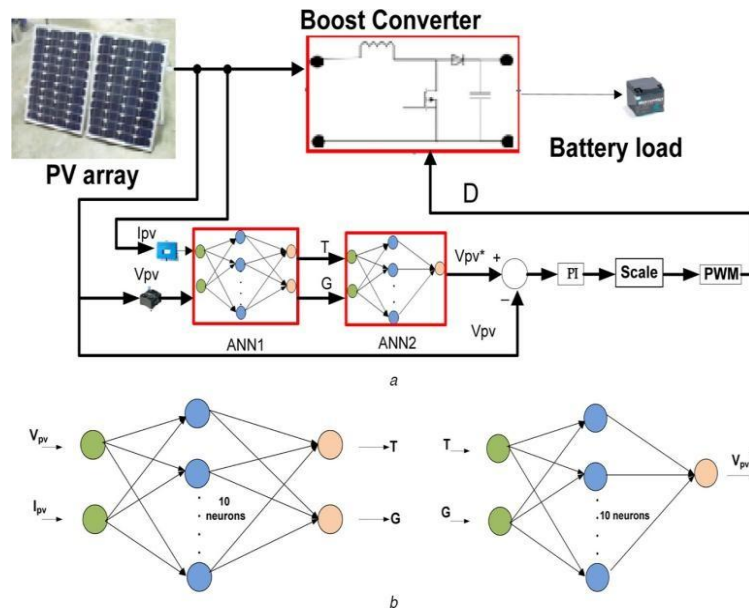


Fig shows4 : MPPT with Artificial Neural Networks (ANN) for Solar-Powered Systems

Once the training of the ANN is completed the neuron weights are to be specified such as the V_{mpp} is the output of the ANN for the input values of T and G . Using the V - I characteristic of the modeled PV, the current at the MPPT I_{mpp} can now be calculated

As a result, multiplying V_{mpp} and I_{mpp} yields maximum power P_{max} .

The PV and the MPPT tracker shown in Fig. 4 are made up of a converter and an ANN-based control unit. The following equation is used to manage a chopper with a particular V_{mpp} and I_{mpp} duty cycle at any given time:

IV. PROPOSED DC-DC CONVERTER

The proposed DC-DC shown in figure 4.1 has four active power switches ($S1$, $S2$, $S3$, and $S4$), two identical inductors ($L1$ and $L2$), a diode ($D1$), and a capacitor (CH) at the high voltage side. Diode $D1$ helps in blocking the reverse voltage V_L appearing across the MOSFET while the switches $S1$ and $S2$ are conducting in boost mode. A switching frequency of f_s is used by the switches $S1$, $S2$, $S3$, and $S4$. During



boost mode, switches S1 and S2 have a duty ratio of d_1 , and switch S3 has a duty ratio of d_2 . The duty ratio

of the switch S4 is $(1-d_1-d_2)$ during boost mode and it is d_b during buck mode of operation of the converter. **society representative for specific requirements.**

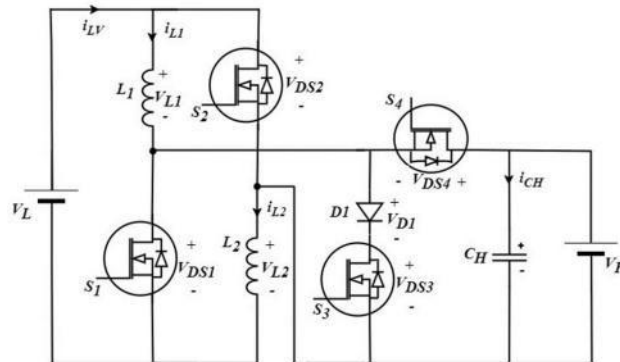


FIGURE 5.1. Proposed high gain bidirectional DC -DC converter

IV.1 OPERATION OF THE DC-DC IN BOOST MODE

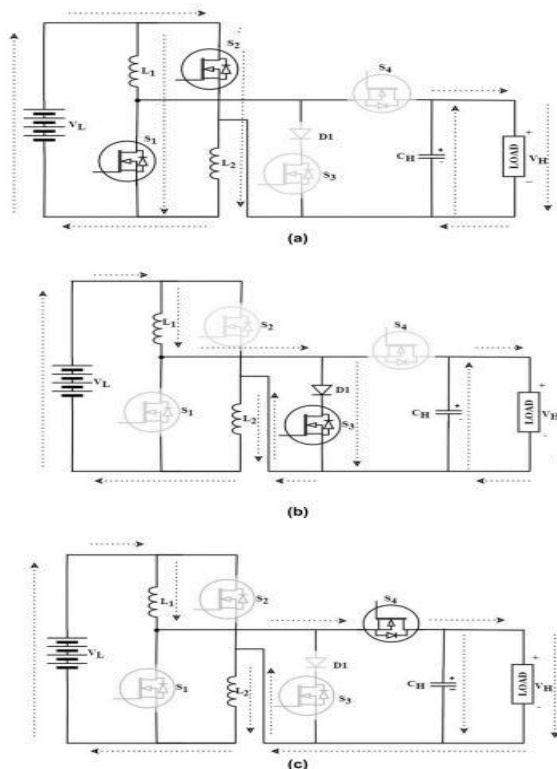
The boost operation of the converter is explained in three different phases namely, Mode I, Mode II and Mode III. The current flow path of the proposed DC-DC operating in boost mode is depicted in figure 5.2. During this mode, the energy is transferred from the low voltage side to the high voltage side of the converter with the help of controlled switches S1, S2, S3 and S4. The switches S1, S2 and S3 are operated through the PWM control. Typical waveforms of the proposed in boost mode for continuous conduction are shown in figure 5.3.



A. Battery Discharging mode:

During this mode, the loads are supplied by two input power sources V_{pv} and V_{bat} . The switches S_1 , S_3 , S_4 are active and feed the power to the load and the switch S_2 is inactive. Every switch has its operation in process of power delivered from source to load. S_1 adjusts the current through the battery to a required value by altering the current through the inductor. The switch S_3 keeps the total output voltage $V_T = V_{pv} + V_{bat}$ at a constant level. The voltage output V_{pv} is also controlled by the switch S_4 . The adjustment of V_T and V_{pv} affects the output voltage V_{bat} . FIGURE 7 represents inductor voltage and current waveforms, as well as the gate signals of switches. There exist four different operation modes in a single switching period

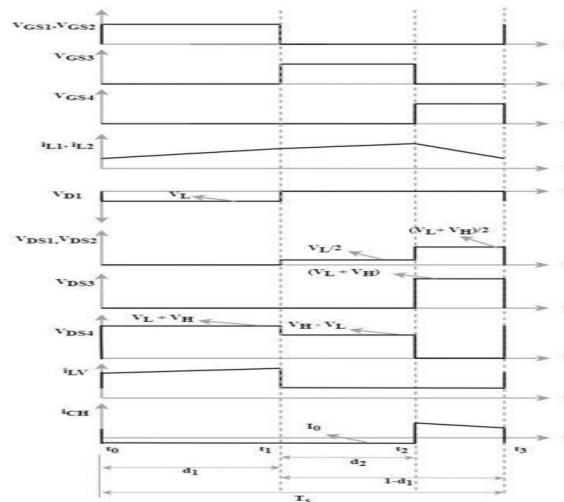
FIGURE 5.2. dc-dc in discharging mode (a) Mode I (b) Mode II (c) Mode III.





Do

FIGURE 5.3. Operational waveforms of in discharging mode



V. BATTERY CHARGING MODE:

During the mode of operation, V_{pv} feeds loads by providing power to V_{bat} . This situation appears in the case where the load-rated power is less and the battery gets charged. During this condition, switches S_1 , S_2 and S_4 are operational, while switch S_3 is inactive. This mode, like the converter in the above mode of operation, takes into account a set duty for each switch. The total output voltage, $V_T = V_{pv} + V_{bat}$ to be adjusted to the appropriate level by turning on S_1 . Switch S_2 keeps the battery charging current (I_{bat}) at a required level. The voltage output V_{pv} is likewise accessed by the switch S_4 . The modification of V_T and V_{pv} controls the voltage output V_{bat} . FIGURE 8 represents the gate switching signals of switches as well as the waveforms representing the voltage and current of the inductor. As per the distinct switch states, the four alternative operating modes exist in one switching period addressed below.

The buck operation of the converter is explained in two different phases during the same switching cycle. The current flow path of the proposed DC-DC operating in buck mode is depicted in figure 5.4. Energy is transferred from the high voltage side to the low voltage side with the help of controlled switches S_4 , S_1 and S_2 in this mode. The switch S_4 is operated through the PWM control with a duty ratio of d_b . Operational waveforms of the proposed DC-DC in buck mode for continuous conduction mode (CCM) are depicted in figure 5.5.

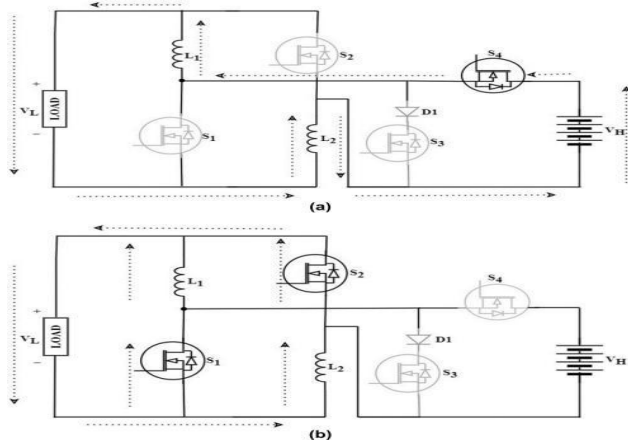
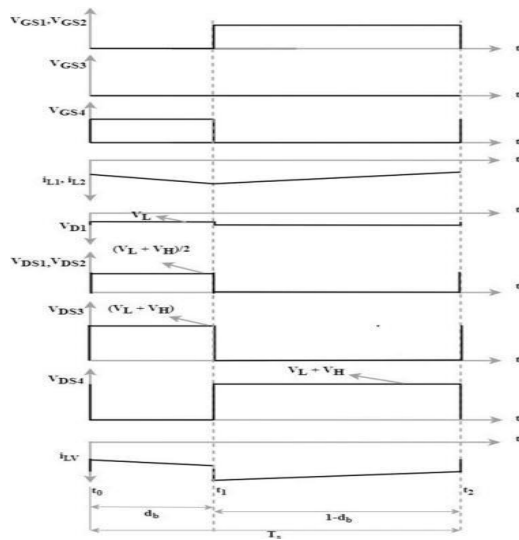


FIGURE 5.4. DC-DC in charging mode (a) Mode I (b) Mode II

FIGURE 5.5 Operational waveforms of DC-DC in discharging mode



1) *Switching Condition 1* ($0 < t < D T$):



During this mode of operation, switch S_1 is inactive, while switch S_3 is still turned off with the switch S_4 is active. The diode D_2 is in reverse bias. FIGURE 6(c) represents the analogous circuit model of the developed converter. The inductor gets discharged by storing the energy which can be distributed to the load with C_1 and R_1 leading to a decrease in inductor current. In this condition, the capacitor C_1 is getting charged, while C_2 is discharged, supplying the energy stored to the load resistance

Switching Condition 2 ($D_1T < t < D_2T$) the circuit of the developed converter. Since the inductor current falls over this period, and inductor distributes its energy stored to the battery V_{bat} . The capacitors C_1 and C_2 are discharged in this mode, delivering the energy stored to R_1 and R_2 load resistances respectively

1) VI.RESULTS AND DISCUSSION

2) *Simulation Results:*

The performance of the developed converter is analyzed and designed using MATLAB software. The simulation parameters of the developed converter are shown in TABLE 2. $V_{pv} = 35V$, $V_{bat} = 48V$ are the input voltage sources. The battery model is utilized as an input source in simulation 2. The converter's output voltages should be regulated at $V_{1ref} = 80V$ and $V_{2ref} = 40V$. Hence, the total output voltage should be able to regulate at $V_{Tref} = 120V$. In addition, for battery discharge and charging modes, battery current should be regulated at $I_{bref} = 3A$ and $I_{bref} = 0.9A$, respectively. For the battery draining and charging modes R_1

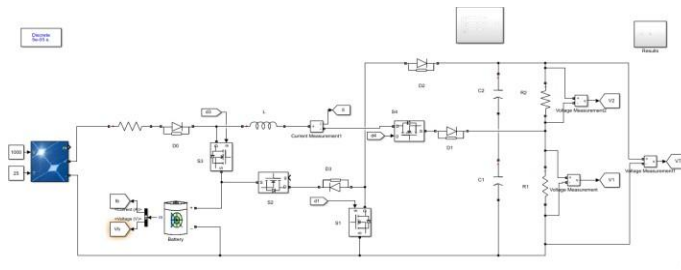


Fig shows6 Simulink Model of the proposed operating in discharging mode

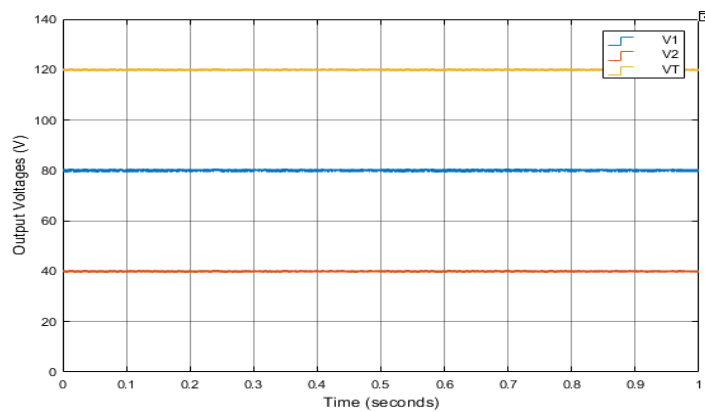


FIGURE 6.1. Output voltages in battery discharging mode

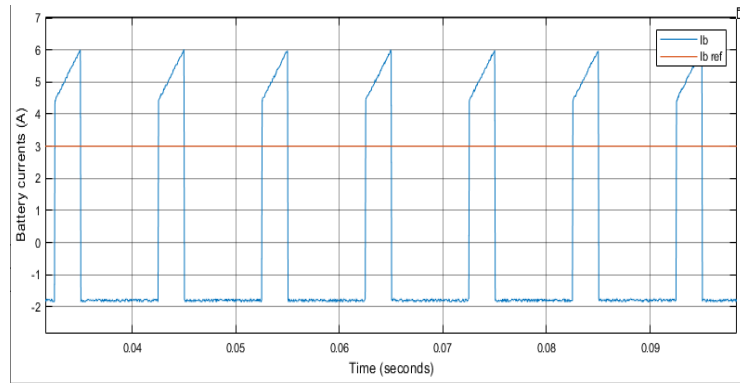


FIG 6.2Battery Current and Reference Battery current in Discharging Mode

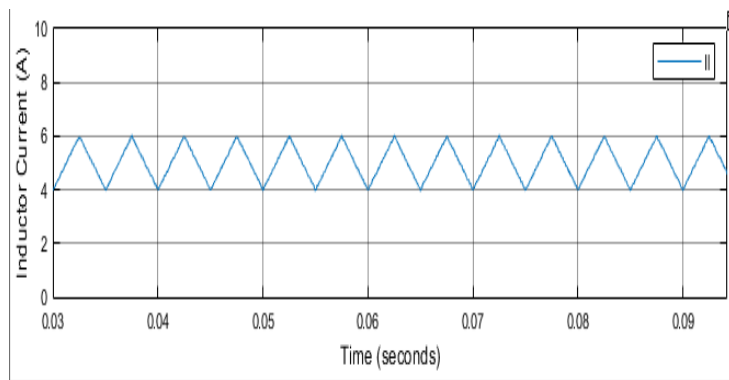


FIG 6.3Inductor Current in discharging Mode



This case study presents a MATLAB/Simulink-based simulation of a proposed dual input DC-DC converter designed for electric vehicle (EV) systems powered by renewable energy. The converter topology integrates two energy sources—a photovoltaic (PV) module and a battery—feeding a resistive load through a multi-switch converter network. The objective of this study is to validate the converter's ability to effectively manage power flow, maintain voltage stability, and support charging and discharging operations.

The simulation model features a PV source connected via a diode and a switch network (S3) with a shared inductor (L) to facilitate energy transfer. The battery is interfaced through another controlled switch (S2), and both inputs are merged and routed through a common path to the load. A set of switches and diodes (S1, S4, D1-D4) in combination with capacitors (C1, C2) and resistive loads (R1, R2) are employed to manage power delivery and voltage regulation.

Control blocks manage the duty cycle and timing of switches to ensure proper operation in different modes:

- Battery Charging Mode (PV powers load and charges battery)
- Battery Discharging Mode (Battery and PV supply power together)
-

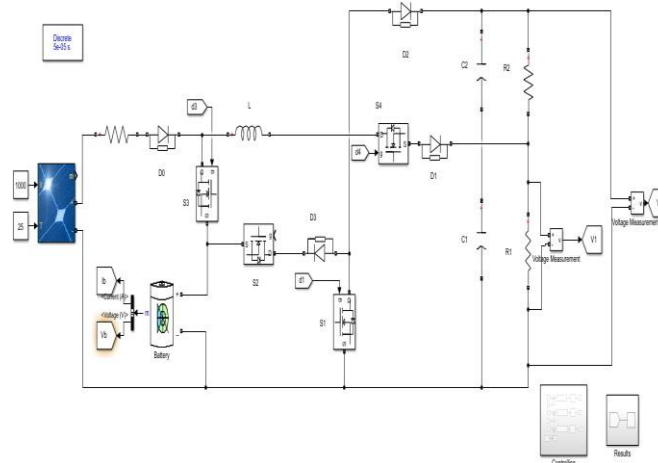
Voltage and current measurements are monitored at various points, especially at the load terminals, using embedded scopes and sensors (V1, VT) to assess system response.

The simulation results confirm the efficiency, dynamic response, and voltage stability of the converter under varying conditions. This proves the feasibility and effectiveness of the proposed converter in a real-world EV scenario with hybrid energy sources

[1] Simulink Model of Figure-6.7

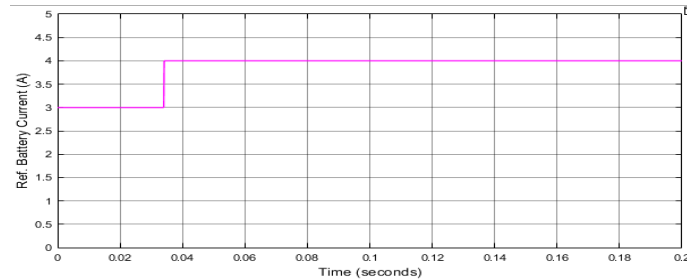
[2] Simulink Model of Figure-6.7

[3] Simulink Model of Figure-6.7





Simulink Model of Figure-6.7



6.8 Change in Battery Reference Current

Case Study: Charging Mode Operation of Proposed Dual Input DC-DC Converter

In the charging mode, the proposed dual input DC-DC converter is designed to allow the photovoltaic (PV) source to simultaneously supply power to the load and charge the battery. This operational mode plays a crucial role in energy-efficient electric vehicle (EV) systems, especially when solar energy is available in abundance.

From the simulation model, when the PV module generates power under sufficient irradiance and temperature, switch S3 is activated, allowing current to flow from the PV to both the load and the battery charging path. Switch S2 remains off during this period, isolating the battery from discharging. The inductor (L) helps in smoothing the current flow, and diode D0 prevents backflow toward the PV source.

[4] Energy is routed through diodes D1 and D3, and capacitors C1 and C2 act as energy buffers, maintaining voltage stability and reducing ripple. The current splits between the load (via R1 and R2) and the battery path, enabling simultaneous operation. The measured output voltage at the load remains consistent, and the battery receives a charging current without significant oscillations or drops in system voltage.

[5] This mode demonstrates the converter's intelligent energy management and proves its ability to harness solar energy effectively while maintaining system efficiency and battery health. The results confirm that the converter meets operational requirements during charging, making it a reliable component in EV power architectures.

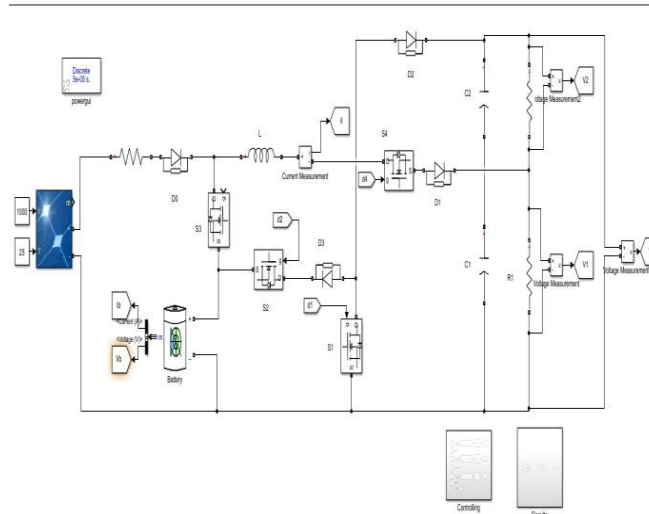


FIG 6.9 Simulink Model in Charging Mode

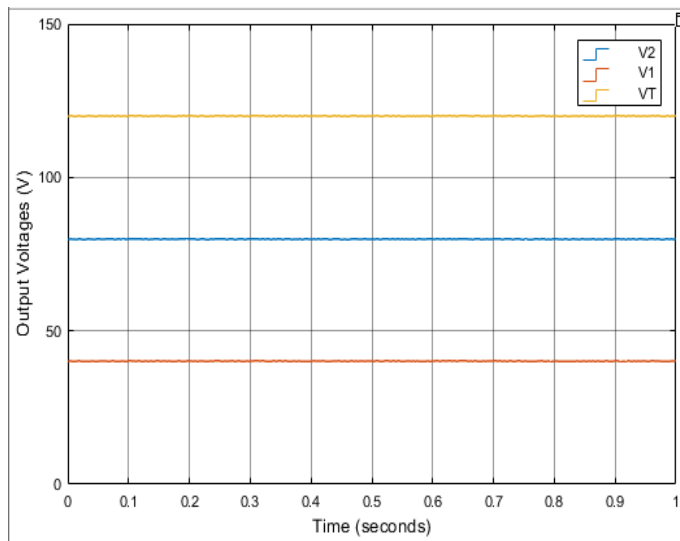


FIG 6.10 Output Voltages in charging mode

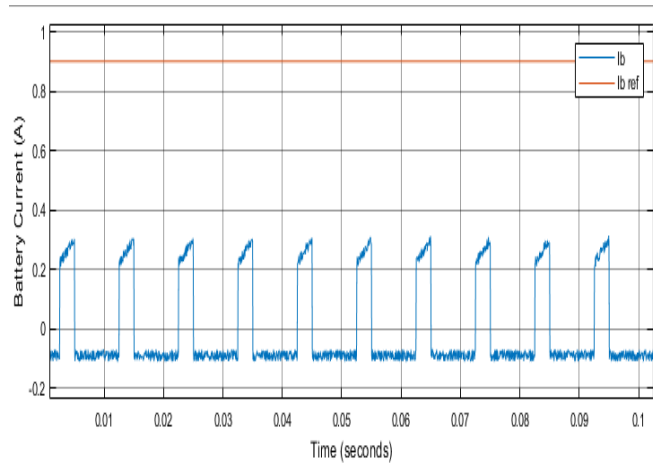


FIG 6.11Battery Current and Reference Battery Current

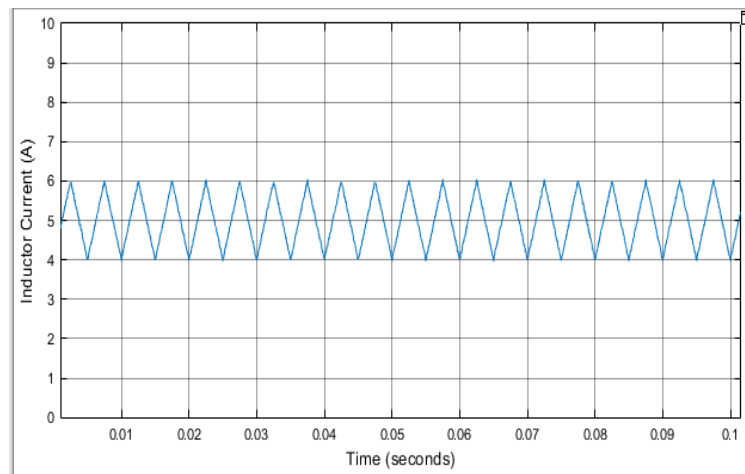


FIG 6.12Inductor Current

Case Study: Reference Battery Current Operation in Dual Input DC-DC Converter

In this case study, we examine the behavior of the reference battery current during the operation of the proposed dual input DC-DC converter. The primary goal is to regulate battery charging or discharging current according to the system's demand, ensuring both energy balance and battery safety.

In the simulation model, the reference current is controlled dynamically based on real-time measurements of PV output and load requirements. The battery current (I_b) is monitored and compared with a predefined reference current (I_{ref}). Based on the error between these two, control signals are generated to appropriately switch S2 and S3, determining whether the battery charges or discharges.



When the PV source generates excess power, the controller commands S3 to conduct, allowing current to flow into the battery, thereby charging it. The battery current follows the reference closely, indicating accurate tracking and regulation. Conversely, during low solar irradiance or high load demand, S2 is activated, enabling battery discharge to supplement the PV power.

The results show a smooth transition and excellent current regulation performance, where the actual battery current effectively tracks the reference signal. This highlights the converter's capability to manage bidirectional energy flow, a vital feature in smart EV energy systems and renewable-integrated microgrids. Overall, this case confirms the efficiency and reliability of the current control strategy used in the proposed converter, making it well-suited for applications requiring precise battery management.

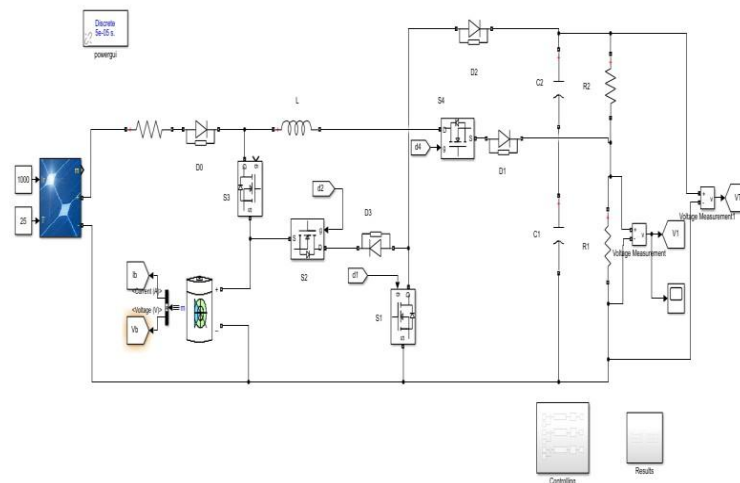


FIG 6.13 Simulink Model of change in reference battery current

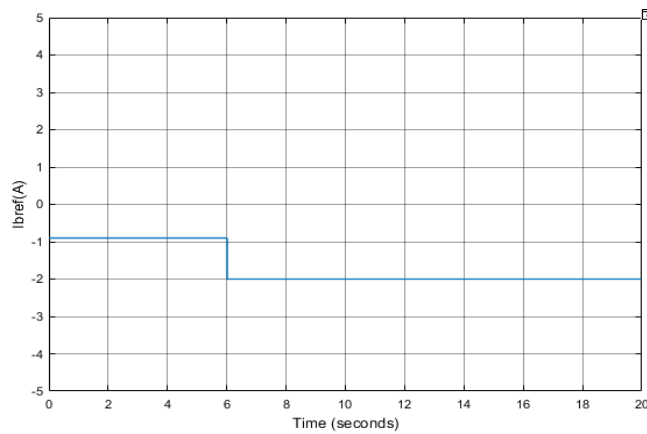


FIG 6.14 Change in reference battery current

Case Study: Discharging Mode of the Proposed Dual Input DC-DC Converter

In the discharging mode, the system utilizes the stored energy from the battery to support the load or motor



drive when the solar PV input is insufficient or unavailable. This mode is particularly critical during low irradiance periods, such as cloudy weather or nighttime, ensuring uninterrupted energy supply to the system.

As shown in the diagram:

- The battery serves as the active input, while the PV panel either contributes minimally or is bypassed.
- The converter operates with switch S2 activated, allowing current to flow from the battery through the inductor (L) and associated components (D3, S1, D1) toward the output.
- The controlled switching ensures that the energy is efficiently transferred, maintaining the required DC link voltage to feed the motor drive.
- The voltage and current measurements are continuously monitored to regulate output and protect components from overcurrent or overvoltage conditions.
- On the output side, an inverter stage (shown with gates and decoder blocks) converts the regulated DC into three-phase AC power suitable for driving the BLDC motor.
- The motor performance is observed via indicators like stator current, rotor speed, and electromagnetic torque, reflecting the effectiveness of power transfer during discharge.

This case study demonstrates that in discharging mode, the battery seamlessly compensates for the lack of solar energy, ensuring that the motor load continues to operate efficiently. The system exhibits robust performance and adaptability, essential for applications in electric vehicles and hybrid renewable systems, where dependable energy flow is vital.

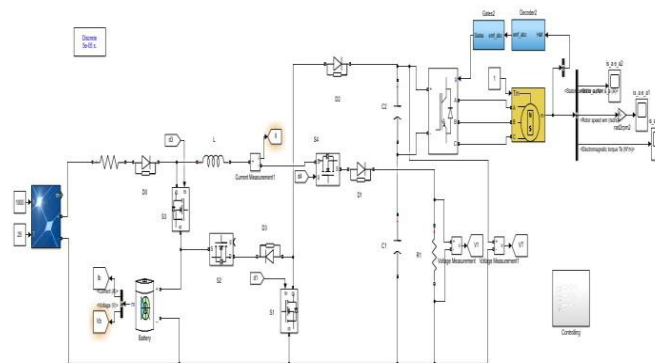


FIG 6.15 Simulink Model of Electric Vehicle connected to a system in discharging mode

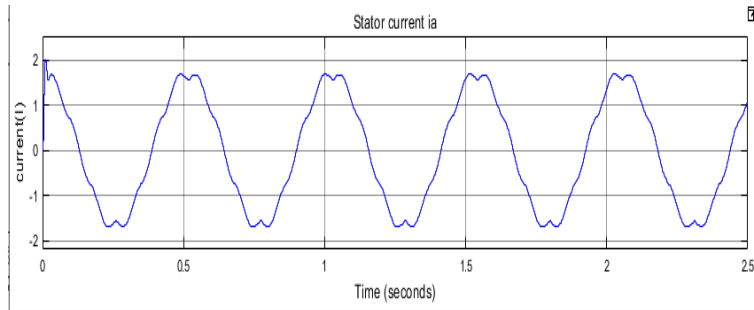
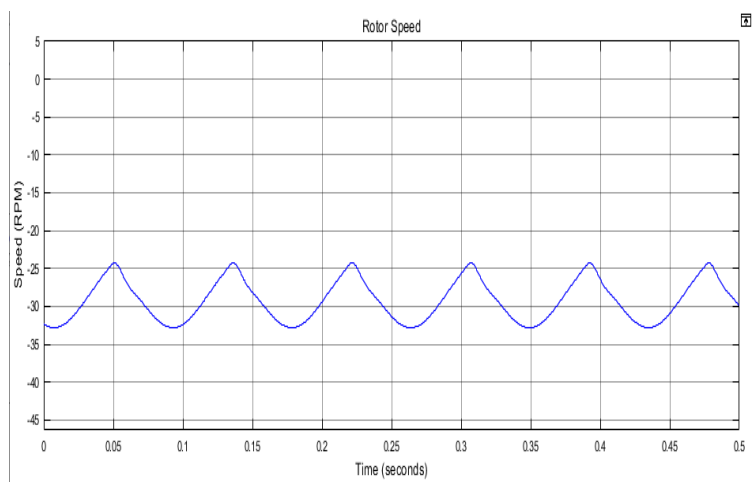


FIG 6.16 Stator Current

FIG 6.17 Rotor Speed



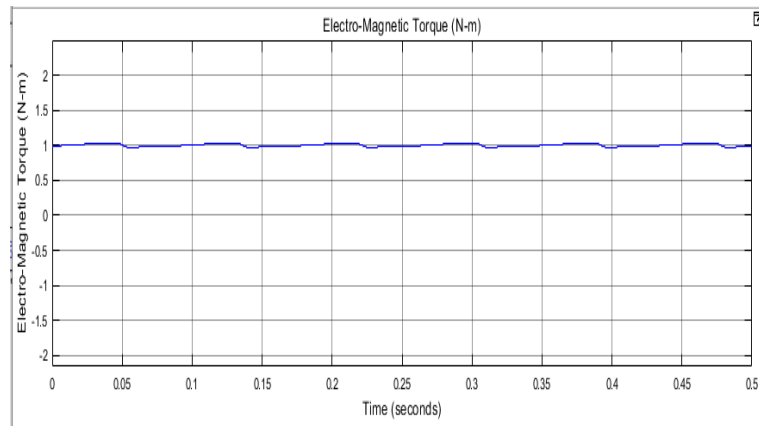


FIG 6.18Electro-Magnetic Torque

case Study: Charging Mode of the Proposed System in Electric Vehicle Application

In charging mode, the Simulink model demonstrates the operation of a photovoltaic (PV) integrated dual input DC-DC converter system connected to an electric vehicle (EV) battery. This mode becomes active when solar energy is available and sufficient to charge the battery while possibly powering the load simultaneously.

Key Observations from the Model:

- The solar PV panel is the primary energy source, supplying power to both the battery and the DC link.
- Switch S3 and diode D0 are activated to direct the solar energy into the charging circuit.
- The inductor (L) and the DC-DC converter stages (comprising switches S2 and S1, and diodes D3 and D1) manage the controlled energy flow toward the battery.
- The battery charging current is regulated using appropriate control strategies to prevent overcharging and ensure optimal battery health.
- The system also supports simultaneous load operation, with the inverter section converting DC to three-phase AC to power the BLDC motor.



- The system also supports simultaneous load operation, with the inverter section converting DC to three-phase AC to power the BLDC motor.
- The motor behavior is monitored via measurements of stator current, rotor speed, and electromagnetic torque, ensuring system performance is not compromised during charging.
- The voltage measurement blocks confirm stable and safe voltage levels across different sections of the system.

This case study highlights that the proposed system supports dual-mode operation, with efficient power sharing between battery charging and motor operation. In charging mode, it maximizes the utilization of renewable solar energy, promoting sustainability and energy independence for electric vehicle applications.

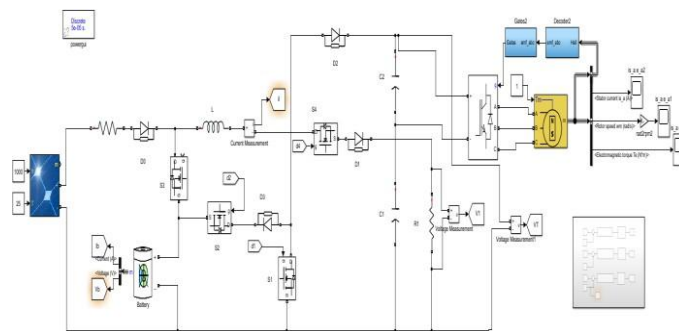


FIG 6.19 Simulink Model of Electric Vehicle connected to a system in charging mode

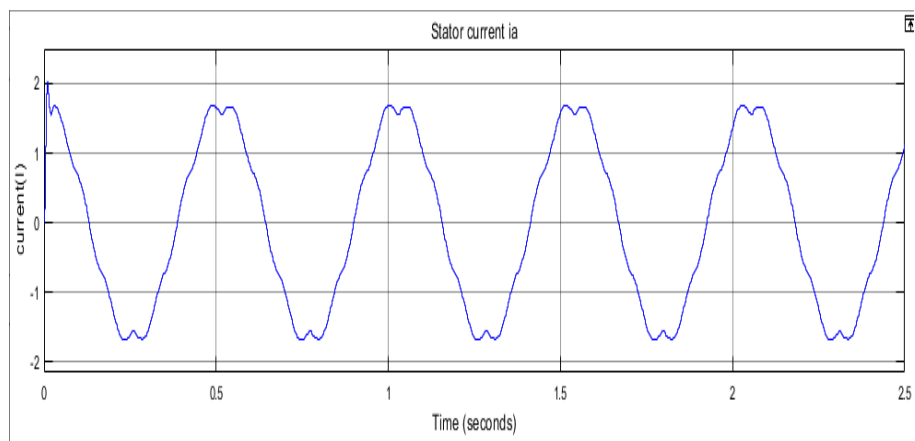




FIG 6.20 Stator Current

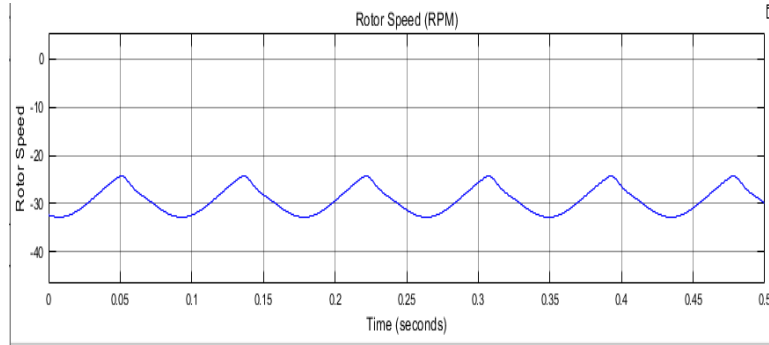


FIG 6.21 Rotor Speed

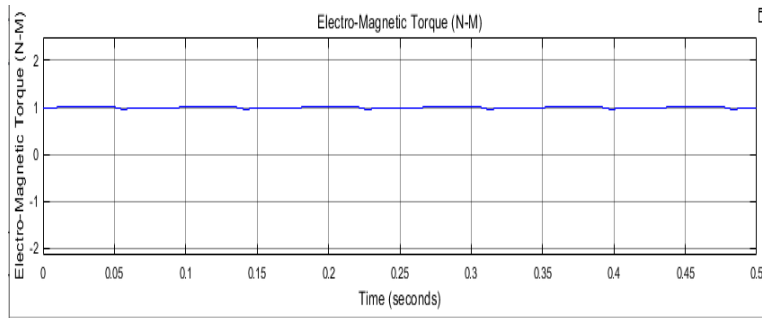


FIG 6.22 Electro-Magnetic Torque

CONCLUSION

This study has successfully presented the design, modeling, and control of a novel single-inductor, non-isolated, multi-port DC-DC converter for electric vehicle (EV) applications. The proposed converter efficiently integrates multiple energy sources—primarily solar photovoltaic (PV) and battery storage—to provide reliable dual-output power for high- and low-voltage EV subsystems. Its simplified architecture, using only one inductor and a limited number of switches and diodes, makes it compact, cost-effective, and well-suited for real-world deployment in EV systems.

By supporting both battery charging and discharging modes, the converter ensures uninterrupted energy



supply under varying solar conditions. Advanced control strategies and compensators were implemented to regulate output voltages and battery currents, achieving accurate tracking of reference signals. Both simulation in MATLAB/Simulink and hardware validation confirmed the converter's robust dynamic performance, fast transient response, and system stability.

Overall, the proposed converter offers a promising solution for hybrid energy management in electric vehicles, enabling sustainable, efficient, and flexible power delivery, and paving the way for smarter renewable energy integration in transportation systems.

REFERENCES [1]

- [1] S. R. Khasim and C. Dhanamjayulu, "Selection parameters and synthesis of multi-input converters for electric vehicles: An overview," *Renew. Sustain. Energy Rev.*, vol. 141, May 2021, Art. no. 110804, doi: [10.1016/j.rser.2021.110804](https://doi.org/10.1016/j.rser.2021.110804).
- [2] P.-J. Liu, Y.-K. Lo, H.-J. Chiu, and Y.-J. Emery Chen, "Dual-current pump module for transient improvement of step-down DC-DC converters," *IEEE Trans. Power Electron.*, vol. 24, no. 4, pp. 985–990, Apr. 2009, doi: [10.1109/TPEL.2008.2010322](https://doi.org/10.1109/TPEL.2008.2010322).
- [3] J. Macaulay and Z. Zhou, "A fuzzy logical-based variable step size P&O MPPT algorithm for photovoltaic system," *Energies*, vol. 11, no. 6, p. 1340, May 2018, doi: [10.3390/en11061340](https://doi.org/10.3390/en11061340).
- [4] M. Dhananjaya, D. Ponuru, T. S. Babu, B. Aljafari, and H. H. Alhelou, "A new multi-output DC-DC converter for electric vehicle application," *IEEE Access*, vol. 10, pp. 19072–19082, 2022.
- [5] L. Wang, E. G. Collins, and H. Li, "Optimal design and real-time control for energy management in electric vehicles," *IEEE Trans. Veh. Technol.*, vol. 60, no. 4, pp. 1419–1429, May 2011, doi: [10.1109/TVT.2011.2122272](https://doi.org/10.1109/TVT.2011.2122272).
- [6] M. Zandi, A. Payman, J. P. Martin, S. Pierfederici, B. Davat, and F. Meibody-Tabar, "Energy management of a fuel cell/supercapacitor/ battery power source for electric vehicular applications," *IEEE Trans. Veh. Technol.*, vol. 60, no. 2, pp. 433–443, Nov. 2011, doi: [10.1109/TVT.2010.2091433](https://doi.org/10.1109/TVT.2010.2091433).
- [7] K. Suresh, C. Bharatiraja, N. Chellammal, M. Tariq, R. K. Chakraborty, M. J. Ryan, and B. Alamri, "A multifunctional non-isolated dual input-dual output converter for electric vehicle applications," *IEEE Access*, vol. 9, pp. 64445–64460, 2021.



REFERENCES [1]

- [1] S. R. Khasim and C. Dhanamjayulu, "Selection parameters and synthesis of multi-input converters for electric vehicles: An overview," *Renew. Sustain. Energy Rev.*, vol. 141, May 2021, Art. no. 110804, doi: [10.1016/j.rser.2021.110804](https://doi.org/10.1016/j.rser.2021.110804).
- [2] P.-J. Liu, Y.-K. Lo, H.-J. Chiu, and Y.-J. Emery Chen, "Dual-current pump module for transient improvement of step-down DC–DC converters," *IEEE Trans. Power Electron.*, vol. 24, no. 4, pp. 985–990, Apr. 2009, doi: [10.1109/TPEL.2008.2010322](https://doi.org/10.1109/TPEL.2008.2010322).
- [3] J. Macaulay and Z. Zhou, "A fuzzy logical-based variable step size P&O MPPT algorithm for photovoltaic system," *Energies*, vol. 11, no. 6, p. 1340, May 2018, doi: [10.3390/en11061340](https://doi.org/10.3390/en11061340).
- [4] M. Dhananjaya, D. Ponuru, T. S. Babu, B. Aljafari, and H. H. Alhelou, "A new multi-output DC–DC converter for electric vehicle application," *IEEE Access*, vol. 10, pp. 19072–19082, 2022.
- [5] L. Wang, E. G. Collins, and H. Li, "Optimal design and real-time control for energy management in electric vehicles," *IEEE Trans. Veh. Technol.*, vol. 60, no. 4, pp. 1419–1429, May 2011, doi: [10.1109/TVT.2011.2122272](https://doi.org/10.1109/TVT.2011.2122272).
- [6] M. Zandi, A. Payman, J. P. Martin, S. Pierfederici, B. Davat, and F. Meibody-Tabar, "Energy management of a fuel cell/supercapacitor/ battery power source for electric vehicular applications," *IEEE Trans. Veh. Technol.*, vol. 60, no. 2, pp. 433–443, Nov. 2011, doi: [10.1109/TVT.2010.2091433](https://doi.org/10.1109/TVT.2010.2091433).
- [7] K. Suresh, C. Bharatiraja, N. Chellammal, M. Tariq, R. K. Chakraborty, M. J. Ryan, and B. Alamri, "A multifunctional non-isolated dual input-dual output converter for electric vehicle applications," *IEEE Access*, vol. 9, pp. 64445–64460, 2021.
- [8] S. R. Khasim and C. Dhanamjayulu, "Design and implementation of asymmetrical multilevel inverter with reduced components and low voltage stress," *IEEE Access*, vol. 10, pp. 3495–3511, 2022, doi: [10.1109/ACCESS.2022.3140354](https://doi.org/10.1109/ACCESS.2022.3140354).
- [9] A. Ajami, H. Ardi, and A. Farakhor, "A novel high step-up DC/DC converter based on integrating coupled inductor and switched-capacitor techniques for renewable energy applications," *IEEE Trans. Power Electron.*, vol. 30, no. 8, pp. 4255–4263, Aug. 2015, doi: [10.1109/TPEL.2014.2360495](https://doi.org/10.1109/TPEL.2014.2360495).
- [10] M. R. Banaei, H. Ardi, R. Alizadeh, and A. Farakhor, "Non-isolated multi-input-single-output DC/DC converter for photovoltaic power generation systems," *IET Power Electron.*, vol. 7, no. 11, pp. 2806–2816, Nov. 2014, doi: [10.1049/iet-pel.2013.0977](https://doi.org/10.1049/iet-pel.2013.0977).
- [11] O. Hegazy, R. Barrero, J. Van Mierlo, P. Lataire, N. Omar, and T. Coosemans, "An advanced power electronics interface for electric vehicles applications," *IEEE Trans. Power Electron.*, vol. 28, no. 12, pp. 5508–5521, Dec. 2013, doi: [10.1109/TPEL.2013.2256469](https://doi.org/10.1109/TPEL.2013.2256469).
- [12] C. Dhanamjayulu, S. Padmanaban, V. K. Ramachandaramurthy,



- J. B. Holm-Nielsen, and F. Blaabjerg, “Design and implementation of multilevel inverters for electric vehicles,” *IEEE Access*, vol. 9, pp. 317–338, 2021.
- [13] Y. Cao and J. A. Abu Qahouq, “Evaluation of bi-directional single-inductor multi-input battery system with state-of-charge balancing control,” *IET Power Electron.*, vol. 11, no. 13, pp. 2140–2150, Nov. 2018.
- [14] S. R. Khasim, D. C, S. Padmanaban, J. B. Holm-Nielsen, and M. Mitolo, “A novel asymmetrical 21-level inverter for solar PV energy system with reduced switch count,” *IEEE Access*, vol. 9, pp. 11761–11775, 2021, doi: [10.1109/ACCESS.2021.3051039](https://doi.org/10.1109/ACCESS.2021.3051039).
- [15] R. Ahmadi and M. Ferdowsi, “Double-input converters based on H-bridge cells: Derivation, small-signal modeling, and power sharing analysis,” *IEEE Trans. Circuits Syst. I, Reg. Papers*, vol. 59, no. 4, pp. 875–888, Apr. 2012, doi: [10.1109/TCSI.2011.2169910](https://doi.org/10.1109/TCSI.2011.2169910).
- [16] L. Solero, A. Lidozzi, and J. A. Pomilio, “Design of multiple-input power converter for hybrid vehicles,” *IEEE Trans. Power Electron.*, vol. 20, no. 5, pp. 1007–1016, Sep. 2005, doi: [10.1109/TPEL.2005.854020](https://doi.org/10.1109/TPEL.2005.854020).
- [17] B. Faridpak, M. Farrokhifar, M. Nasiri, A. Alahyari, and N. Sadoogi, “Developing a super-lift Luo-converter with integration of buck converters for electric vehicle applications,” *CSEE J. Power Energy Syst.*, vol. 7, no. 4, pp. 811–820, 2020.
- [18] S. R. Khasim and D. C, “Design of multiple input DC–DC converters for interfacing solar/fuel cell/battery electric vehicles,” in *Proc. Innov. Power Adv. Comput. Technol. (i-PACT)*, Nov. 2021, pp. 1–7.
- [19] C. Dhanamjayulu, S. R. Khasim, S. Padmanaban, G. Arunkumar, J. B. Holm-Nielsen, and F. Blaabjerg, “Design and implementation of multilevel inverters for fuel cell energy conversion system,” *IEEE Access*, vol. 8, pp. 183690–183707, 2020, doi: [10.1109/access.2020.3029153](https://doi.org/10.1109/access.2020.3029153).
- [20] K. Suresh, N. Chellammal, C. Bharatiraja, P. Sanjeevikumar, F. Blaabjerg, and J. B. H. Nielsen, “Cost-efficient nonisolated three-port DC–DC converter for EV/HEV applications with energy storage,” *Int. Trans. Electr. Energy Syst.*, vol. 29, no. 10, p. e12088, Oct. 2019.